Progress In Electromagnetics Research, PIER 62, 217–235, 2006

DEVELOPMENT AND ANALYSIS OF A MICROWAVE DIRECT CONTACT WATER-LOADED BOX-HORN APPLICATOR FOR THERAPEUTIC HEATING OF BIO-MEDIUM

R. C. Gupta and S. P. Singh

Department of Electronics Engineering
Institute of Technology
Banaras Hindu University
Varanasi-221 005, U.P., India

Abstract—A novel, potential and efficient microwave direct contact hyperthermia applicator referred to as water-loaded box-horn for therapeutic heating of bio-medium is designed and developed at 915 and 2450 MHz. Also, theoretical expressions for fields in bio-medium as produced by a direct contact box-horn applicator have been derived using plane wave spectral technique. The box-horn is a special type of dual mode horn antenna which supports TE_{10}- and TE_{30}-modes. Therefore, the aperture field distribution over the H-plane of the box-horn is nearly uniform which prevents steep temperature gradients in the heating medium. Water-loading of the box-horn provides a better impedance match to the bio-medium and hence better coupling of microwave energy into bio-medium. Also, it reduces the size of box-horn applicator considerably. The SAR distributions in bio-medium in direct contact with water-loaded box-horn have been computed theoretically with the developed analytical model and measured experimentally with the help of Agilent/HP vector network analyzer (8714 ET) at 915 and 2450 MHz. The theoretical and experimental results for SAR are in nearly in agreement with each other. It is investigated that higher penetration depth, lower power absorption coefficient and higher half-power width/depth or lower resolution in heating medium are found for box-horn designed at 915 MHz in comparison to those for box-horn designed at 2450 MHz.

1. INTRODUCTION

Emerging application of microwave in hyperthermia treatment of cancer demands challenging characteristics of applicator. The applicator must be designed to elevate the temperature uniformly throughout the tumor to the therapeutic temperature range (43° to 50°C). The applicator must be light weight and compact. It should be simple and as small as possible for a specified aperture size to facilitate its clinical use. When the applicator is in direct contact with phantom tissue, the leakage around it should be as small as possible. These requirements, put together provide a challenging list of specifications that demand innovation in applicator design beyond known conventional applicators.

A number of investigations have been carried out on several types of direct contact applicators for hyperthermia treatment of cancer. Rectangular/circular waveguide applicators [1–4], multimodal applicator [5], conical horn antenna [6], dielectric lens/slab-loaded waveguide [7–9] etc. as direct contact hyperthermia applicators have been reported in the literature. The type of applicator selected depends on the production of sufficient thermal field distributions at different depths of the tumor in a variety of anatomical sites. For minimum microwave exposure to the operator as well as unprescribed tissues of patient, direct contact applicators are desirable instead of spaced applicators. They are inherently safer as they can readily reduce unwanted radiation. For superficial tumors, single contact applicators at 915 and 2450 MHz have been used to treat well localized tumors extending upto a depth of 3 cm. Waveguide and horn antennas are also put under this category of hyperthermia applicators. Higher penetration depth can be achieved by either employing an applicator operating at a lower frequency or by using several applicators as a phased array. For uniform heating of these tumors properly designed multimode waveguide/horn can be used.

In this paper, the authors have proposed a novel, potential and efficient direct contact water-loaded box-horn applicator for hyperthermia treatment of cancer. The box-horn consists of a TE_{10}-mode H-plane sectoral-horn coupled to a length L of rectangular waveguide of same E-plane height but whose H-plane width is large enough to support TE_{30}-mode also. Thus, box-horn is a dual-mode applicator which supports TE_{10}- and TE_{30}-modes. The electric field distribution over the H-plane of the box-horn aperture is nearly uniform which prevents steep temperature gradient in the heating medium. To demonstrate the technical feasibility for a safe and effective design, a prototype direct contact water-loaded box-

horn applicator operating at ISM (Industrial, Scientific and Medical) frequencies of 915 and 2450 MHz have been designed and developed. The water-loading of the box-horn reduces any mismatch resulting from bio-medium since the dielectric permittivity of the bio-medium is close to that of water. Hence, strong power coupling to the bio-medium can easily be achieved and radiation leakage around the applicator minimized. Moreover, rather high value of the real part of water permittivity ($\varepsilon_w \cong 78$) permits a considerable reduction (by a factor of $\cong 9$) in applicator aperture dimensions, which is very important in trying to make the whole system manageable in phased array application. Analytical model for fields in bio-medium illuminated by the water-loaded box-horn applicator have also been developed using plane wave spectra technique for calculating the heating patterns in planar stratified tissue. The field components numerically evaluated with the help of MATLAB® software may be used to select an aperture size of box-horn to provide the best subcutaneous heating patterns in the tissue. The spatial distribution of specific absorption rate (SAR) or the rate of heating in a planar heating-medium (synthetic muscle) produced by a direct-contact water-loaded box-horn applicator is computed theoretically using developed analytical model and measured experimentally with the help of Agilent/HP vector network analyzer (8714ET) at 915 and 2450 MHz. Other parameters of interest, such as penetration depth, power absorption coefficient and half-power width/depth or resolution in heating medium are also determined theoretically and experimentally at 915 and 2450 MHz for characterizing the water-loaded box-horn applicator. The theoretical and experimental results are found to be nearly in agreement with each other which validate the developed analytical model.

2. THEORETICAL CONSIDERATIONS ON WAVE PROPAGATION IN BIO-MEDIUM

A water-loaded box-horn terminated in bio-medium (synthetic muscle layer) is shown in Fig. 1. The narrow and broad dimensions of the aperture of the box-horn are denoted as a and b respectively. The length of box-horn along z-direction is denoted as L. In present analysis, the muscle layer is considered to be of finite thickness (t_1) followed by infinite free-space layer. Muscle and free-space layers have complex permittivities of ε_1^* and ε_2^* respectively. The analysis of fields in the bi-layered media presented here follows the plane wave spectral technique discussed by Compton [10] and Harrington [11]. It is assumed that box-horn has conducting ground plane extending upto infinity surrounding the box-horn aperture in xy-plane so that

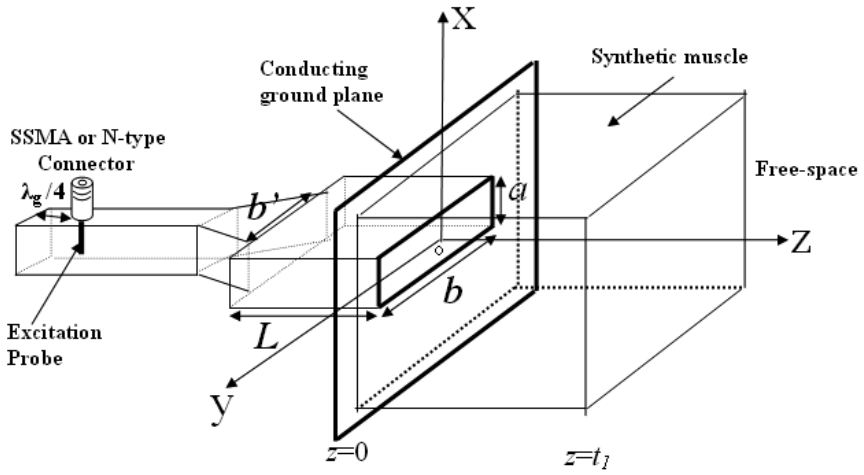

Figure 1. Prototype water-loaded box-horn applicator in direct contact with bio-medium.

the fringe field outside the aperture in xy-plane becomes zero. Many evanescent modes may be excited near the discontinuity regions, such as the aperture of the box-horn. Therefore, the fields inside the waveguide ($z < 0$) can be described as the superposition of the incident and reflected TE_{10}- and TE_{30}-mode fields and many evanescent mode fields. In order to compute the field in the $z < 0$ half-space, the field at the $z = 0$ plane is assumed to be known and is taken to be equal to the superposition of incident TE_{10}- and TE_{30}-propagating mode fields and their respective reflected fields [2, 10, 12]. The effect of non-propagating evanescent modes is generally taken to be secondary [2, 10, 12] under the condition of good impedance matching and is neglected in the present study. This assumption is equivalent to Kirchhoff's approximation, which gives satisfactory results in the forward direction [2, 10, 12]. Thus, the x-component of electric field at the aperture of the box-horn [12] is represented by

$$\begin{aligned} E_{x1}(x, y, 0) \;=\; & a_{10}(1 + \Gamma_{10}) \cos\left(\frac{\pi y}{b}\right) e^{-j\beta_{10}L} \\ & + a_{30}(1 + \Gamma_{30}) \cos\left(\frac{3\pi y}{b}\right) e^{-j\beta_{30}L} \end{aligned} \tag{1}$$

where a_{10} and a_{30} are amplitude coefficients, Γ_{10} and Γ_{30} are reflection coefficients at the interface between water-loaded box-horn aperture and bio-medium, and β_{10} and β_{30} are the phase constants for TE_{10}

and TE_{30} modes respectively. With the aperture electric field as given in Eqn. (1), the fields in the bi-layered media are every-where TE to x and TE to y [10, 11]. Hence, the fields may be represented by an electric vector potential

$$\overline{F} = \phi\hat{x} + \psi\hat{y} \tag{2}$$

where ϕ and ψ are both the solutions to the wave equation

$$\left(\nabla^2 + k_{1,2}^2\right)\left\{\begin{array}{c}\psi\\ \phi\end{array}\right\} = 0 \tag{3}$$

where $k_{1,2}$ are respectively the complex propagation constants in the bio-medium (layer 1) and free space (layer 2) respectively. The solutions for ϕ and ψ can be constructed as the sum of a continuous spectrum of eigenvalues, as given by

$$\psi_1(x,y,z) = \frac{1}{(2\pi)^2}\int_{-\infty}^{\infty}\int_{-\infty}^{\infty}\left[I_{\psi 1}e^{-jk_{z1}z} + R_{\psi 1}e^{+jk_{z1}z}\right]e^{-jk_x x}e^{-jk_y y}dk_x dk_y \tag{4}$$

$$\phi_1(x,y,z) = \frac{1}{(2\pi)^2}\int_{-\infty}^{\infty}\int_{-\infty}^{\infty}\left[I_{\phi 1}e^{-jk_{z1}z} + R_{\phi 1}e^{+jk_{z1}z}\right]e^{-jk_x x}e^{-jk_y y}dk_x dk_y \tag{5}$$

$$\psi_2(x,y,z) = \frac{1}{(2\pi)^2}\int_{-\infty}^{\infty}\int_{-\infty}^{\infty}T_{\psi 1}e^{-jk_{z2}}e^{-jk_x x}e^{-jk_y y}dk_x dk_y \tag{6}$$

$$\phi_2(x,y,z) = \frac{1}{(2\pi)^2}\int_{-\infty}^{\infty}\int_{-\infty}^{\infty}T_{\phi 1}e^{-jk_{z2}z}e^{-jk_x x}e^{-jk_y y}dk_x dk_y \tag{7}$$

The electric and magnetic fields in different layers are found from the relations

$$\overline{E} = -\nabla \times \overline{F} \tag{8}$$

$$\overline{H} = \frac{1}{j\omega\mu_0}\left[k_{1,2}^2\overline{F} + \nabla(\nabla\cdot\overline{F})\right] \tag{9}$$

Through the use of spectral technique as discussed by Compton [10] and as given in Harrington [11], spectral integral representations of the fields in different layers are obtained. The x-, y-, and z-components of electric field in the two layers (muscle and free-space) are derived and are given below:

$$E_{x1}(x,y,z) = \frac{1}{(2\pi)^2}\int_{-\infty}^{\infty}\int_{-\infty}^{\infty}\left[-jk_{z1}I_{\psi1}e^{-jk_{z1}z} + jk_{z1}R_{\psi1}e^{+jk_{z1}z}\right] \cdot e^{-jk_x x}e^{-jk_y y}dk_x dk_y \tag{10}$$

$$E_{y1}(x,y,z) = \frac{1}{(2\pi)^2}\int_{-\infty}^{\infty}\int_{-\infty}^{\infty}\left[+jk_{z1}I_{\phi1}e^{-jk_{z1}z} - jk_{z1}R_{\phi1}e^{+jk_{z1}z}\right] \cdot e^{-jk_x x}e^{-jk_y y}dk_x dk_y \tag{11}$$

$$\begin{aligned} E_{z1}(x,y,z) = {} & \frac{1}{(2\pi)^2}\int_{-\infty}^{\infty}\int_{-\infty}^{\infty}\left[I_{\phi1}e^{-jk_{z1}z} + R_{\phi1}e^{+jk_{z1}z}\right] \\ & \cdot e^{-jk_x x}(-jk_y)e^{-jk_y y}dk_x dk_y \\ & -\frac{1}{(2\pi)^2}\int_{-\infty}^{\infty}\int_{-\infty}^{\infty}\left[I_{\psi1}e^{-jk_{z1}z} + R_{\psi1}e^{+jk_{z1}z}\right] \\ & \cdot(-jk_x)e^{-jk_x x}e^{-jk_y y}dk_x dk_y \end{aligned} \tag{12}$$

$$E_{x2}(x,y,z) = \frac{1}{(2\pi)^2}\int_{-\infty}^{\infty}\int_{-\infty}^{\infty} -jk_{z2}T_{\psi1}e^{-jk_{z2}z}e^{-jk_x x}e^{-jk_y y}dk_x dk_y \tag{13}$$

$$E_{y2}(x,y,z) = \frac{1}{(2\pi)^2}\int_{-\infty}^{\infty}\int_{-\infty}^{\infty} +jk_{z2}T_{\phi1}e^{-jk_{z2}z}e^{-jk_x x}e^{-jk_y y}dk_x dk_y \tag{14}$$

$$\begin{aligned} E_{z2}(x,y,z) = {} & \frac{1}{(2\pi)^2}\int_{-\infty}^{\infty}\int_{-\infty}^{\infty} T_{\phi1}e^{-jk_{z2}z}e^{-jk_x x}(-jk_y)e^{-jk_y y}dk_x dk_y \\ & -\frac{1}{(2\pi)^2}\int_{-\infty}^{\infty}\int_{-\infty}^{\infty} T_{\psi1}e^{-jk_{z2}z}(-jk_x)e^{-jk_x x}e^{-jk_y y}dk_x dk_y \end{aligned} \tag{15}$$

where plane wave spectra are $I_{\psi1}$, $I_{\phi1}$, $R_{\psi1}$, $R_{\phi1}$ in muscle layer (layer 1), and $T_{\psi1}, T_{\phi1}$ in free-space (layer 2). It should be noted that $k_{z1} = \sqrt{k_1^2 - k_x^2 - k_y^2}$ and $k_{z2} = \sqrt{k_2^2 - k_x^2 - k_y^2}$.

The equations for the components of H-field can similarly be found by utilizing (4)–(7) and (9). Taking inverse Fourier transform of (10)

and (11) at $z = 0$ gives

$$jk_{z1}[-I_{\psi 1} + R_{\psi 1}] = \frac{4\pi b}{k_x} \sin\left(\frac{k_x a}{2}\right) \cos\left(\frac{k_y b}{2}\right) \cdot \left[\frac{a_{10}(1+\Gamma_{10})e^{-j\beta_{10}L}}{\pi^2 - b^2 k_y^2} - \frac{3a_{30}(1+\Gamma_{30})e^{-j\beta_{30}L}}{9\pi^2 - b^2 k_y^2}\right] \tag{16}$$

and

$$jk_{z1}[I_{\phi 1} - R_{\phi 1}] = 0. \tag{17}$$

Applying the boundary conditions, i.e., the continuity of tangential electric and magnetic fields at $z = t_1$ (the interface between muscle and free-space) gives the necessary remaining four equations as follows:

$$-jk_{z1}I_{\psi 1}e^{-jk_{z1}t_1} + jk_{z1}R_{\psi 1}e^{+jk_{z1}t_1} = -jk_{z2}T_{\psi 1}e^{-jk_{z2}t_1} \tag{18}$$

$$+jk_{z1}I_{\phi 1}e^{-jk_{z1}t_1} - jk_{z1}R_{\phi 1}e^{+jk_{z1}t_1} = +jk_{z2}T_{\phi 1}e^{-jk_{z2}t_1} \tag{19}$$

$$\begin{aligned} &\left(k_1^2 - k_x^2\right)\left[I_{\phi 1}e^{-jk_{z1}t_1} + R_{\phi 1}e^{+jk_{z1}t_1}\right] \\ &\quad -k_x k_y\left[I_{\psi 1}e^{-jk_{z1}t_1} + R_{\psi 1}e^{+jk_{z1}t_1}\right] \\ &= \left(k_2^2 - k_x^2\right)T_{\phi 1}e^{-jk_{z2}t_1} - k_x k_y T_{\psi 1}e^{-jk_{z2}t_1} \end{aligned} \tag{20}$$

$$\begin{aligned} &\left(k_1^2 - k_y^2\right)\left[I_{\psi 1}e^{-jk_{z1}t_1} + R_{\psi 1}e^{+jk_{z1}t_1}\right] \\ &\quad -k_x k_y\left[I_{\phi 1}e^{-jk_{z1}t_1} + R_{\phi 1}e^{+jk_{z1}t_1}\right] \\ &= \left(k_2^2 - k_y^2\right)T_{\psi 1}e^{-jk_{z2}t_1} - k_x k_y T_{\phi 1}e^{-jk_{z2}t_1} \end{aligned} \tag{21}$$

Equations (16) through (21) can be solved for plane wave spectra in different layers. The solution of (16) through (21) is tedious but straight-forward. From Eqs. (16) and (17), R_ψ and R_ϕ can be written as

$$R_{\psi 1} = \frac{m}{jk_{z1}} + I_{\psi 1} \tag{22}$$

where

$$m = \frac{4\pi b}{k_x} \sin\left(\frac{k_x a}{2}\right) \cos\left(\frac{k_y b}{2}\right) \left[\frac{a_{10}(1+\Gamma_{10})e^{-j\beta_{10}L}}{\pi^2 - b^2 k_y^2} - \frac{3a_{30}(1+\Gamma_{30})e^{-j\beta_{30}L}}{9\pi^2 - b^2 k_y^2}\right]$$

and

$$R_{\phi 1} = I_{\phi 1}. \tag{23}$$

The expressions for $R_{\psi 1}$ and $R_{\phi 1}$ obtained from Eqs. (22) and (23) are substituted into Eqs. (18)–(21) and the resulting equations are written in terms of two unknown plane wave spectra $I_{\psi 1}$ and $I_{\phi 1}$. These two resulting equations are solved for $I_{\psi 1}$ and $I_{\phi 1}$ using Cramer's rule. Once the solution for the afore-mentioned plane wave spectra are available, other plane wave spectra $T_{\psi 1}$, $T_{\phi 1}$, $R_{\psi 1}$ and $R_{\phi 1}$ can be determined using Equations (20)–(23). The plane wave spectra $I_{\psi 1}$, $I_{\phi 1}$, $R_{\psi 1}$, $R_{\phi 1}$, $T_{\psi 1}$ and $T_{\phi 1}$ are functions of thickness t_1 of muscle layer, complex propagation constants k_1, and k_2 of the layers, parameters a, b, L, a_{10}, a_{30}, β_{10} and β_{30} of the box-horn and other variables.

The electric field components in x-, y- and z-directions in the bio-medium (muscle layer) can then be found using Eqs. (10) to (12). The total electric field intensity, E_{total1} in the bio-medium, is given by

$$|E_{total1}| = \sqrt{|E_{x1}|^2 + |E_{y1}|^2 + |E_{z1}|^2}. \tag{24}$$

The Specific absorption rate (SAR) in the bio-medium (muscle layer) can be evaluated by

$$SAR = \frac{\sigma_1 |E_{total1}|^2}{2\rho_1} \tag{25}$$

where $\sigma_1 (= \omega \varepsilon_0 \varepsilon_1'')$, ρ_1 and ε_1'' are conductivity, density and imaginary part of relative permittivity of muscle layer respectively.

3. DESIGN AND DEVELOPMENT OF WATER-LOADED BOX-HORN APPLICATOR

The water-loaded box horn is designed as per Silver [12] and then manufactured as hyperthermia applicator using 0.2 cm thick copper sheet. For brevity the design procedure is not included here. To investigate the effect of frequency on SAR values, two box-horns of different dimensions are designed and fabricated at 915 and 2450 MHz. The first water-loaded box-horn is designed and developed to operate at 915 MHz with the dimensions $a = 1.26$ cm, $b = 5.94$ cm, $L = 3.08$ cm and the flare angle of the H-plane sectoral horn exciting the box is $\theta_H = 30^\circ$ in H-plane. In the second design, a water-loaded box-horn is fabricated to operate at 2450 MHz with the dimensions $a = 0.43$ cm, $b = 2.23$ cm, $L = 1.16$ cm and flare angle of the H-plane sectoral horn exciting the box is 30° in H-plane. θ_H is flare angle of H-plane sectoral horn exciting the box in H-plane. θ_H determines the H-plane dimension of the mouth sectoral horn and the ratio of the

H-plane dimensions of the mouth of sectoral horn and box waveguide determines the ratio of the coefficients a_{30} to a_{10}. Therefore, flare angle of the horn in H-plane (θ_H) governs the ratio of a_{30} to a_{10}. For uniform aperture field distribution, optimum efficiency and minimum amplitude taper loss, ratio of a_{30} to a_{10} has been chosen to be 0.3 and the dimension of box-aperture (b) has been taken to be 1.6 λ_w in the design of water-loaded box-horn, for which θ_H is found to be 30° [12]. Here λ_w is the wavelength in water. The permittivity of water [13] has been taken to be $78 - j3.51$ at 915 MHz and $77 - j12.09$ at 2450 MHz for designing the water-loaded box-horn.

In Fig. 1, the perspective view of the developed box-horn applicator is shown. Both the box-horn applicators have sufficient size of conducting ground planes (screens) of copper surrounding the respective apertures in xy-plane so that the fringe field becomes zero. The size of screen is $20 \times 20\,\text{cm}^2$ for box-horn designed at 915 MHz and $15 \times 15\,\text{cm}^2$ for box-horn operating at 2450 MHz. The horns were excited with the help of coaxial probes inserted into the respective built-in TE_{10}-mode input waveguide sections. The probe conductor, connected to the central conductor of a RF-coaxial connector (SSMA or N-type Jack), was extended towards the opposite broad-wall of the waveguide section. SSMA (Sub-SubMiniature version A) type jack connector was used for the box-horn designed at 2450 MHz and N-type (Navy type) jack connector was used for the box-horn operating at 915 MHz. Water loaded box-horns employed EIA WR-112 input waveguide at 915 MHz and EIA WR-34 input waveguide at 2450 MHz. The input end of the waveguide section of H-plane sectoral horn was short-circuited. The mouth end of the each horn was opened in the box of the box-horn. The length of the input waveguide section was chosen equal to 2 cm in the design of both the applicators. The coaxial probe was inserted in the middle of broad-dimension of each input waveguide section at a distance of $\lambda_g/4$ from the short-circuit end, where λ_g is the wavelength in the water-loaded input waveguide section for TE_{10} mode given by the relation

$$\lambda_g \cong \frac{\lambda}{\sqrt{\varepsilon'_w}} \frac{1}{\sqrt{1 - \left(\frac{f_{c10}}{f}\right)^2}}$$

ε'_w is the real part of the complex permittivity of water, λ is the free-space wavelength, $f_{c10} = c/(2a\sqrt{\varepsilon'_w})$ is the TE_{10}-mode cutoff frequency c is the velocity of microwave in free space $= 3 \times 10^8$ m/s), and $f = c/\lambda$ is the microwave frequency.

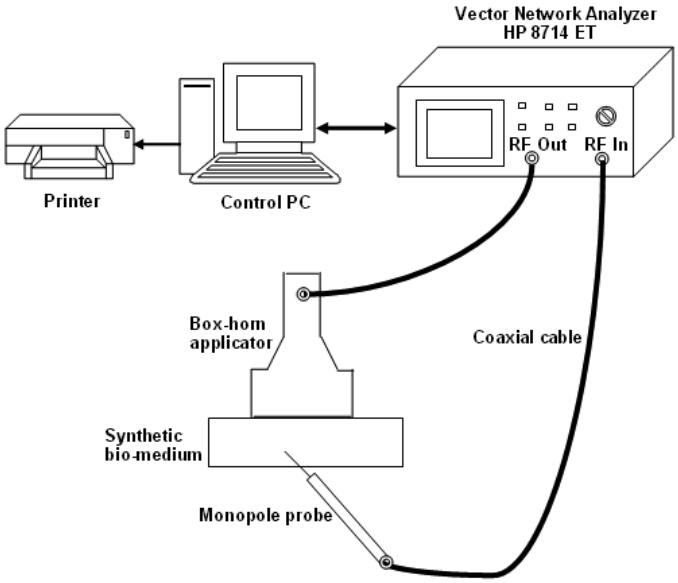

Figure 2. Schematic of the vector network analyzer based tissue characterization system.

4. EXPERIMENTAL TECHNIQUE FOR MEASURING FIELD COMPONENTS IN PHANTOM BIO-MEDIUM

The experimental setup for measuring transmission coefficient (S_{21}-parameter) in phantom bio-medium in direct contact with a box-horn is shown in Fig. 2. The laboratory grade distilled water was used to fill both the box-horns. The S_{21} data can be used to determine SAR-distribution in the synthetic muscle-medium. The planar synthetic muscle was prepared from the material composition given in reference [12] i.e., 30% Gelatin +69% Water +1% NaCl. The complex permittivity of the synthetic muscle-medium was taken to be $51 - j26$ at 915 MHz and $50 - j16$ at 2450 MHz [12]. One of the fabricated box-horns was connected to RF-Out port (Reflection port) of vector network analyzer (Agilent/HP 8714ET) with the help of coaxial cable and a coaxial monopole probe was connected to RF-In port (Transmission port) of the vector network analyzer using flexible coaxial cable. Thus, the power from the vector network analyzer coupled to the box-horn was fed to synthetic muscle in direct contact with the box-horn. The power sensed by the monopole probe inserted at appropriate location in the synthetic muscle is fed back to RF-In port (Transmission port) of the vector network analyzer. The network

analyzer was configured to measure the magnitude of S_{21} parameter (transmission coefficient) in dB with start and stop frequencies of 300 kHz and 3000 MHz respectively. The Marker is set at 915 MHz for measurement with box-horn designed at 915 MHz and at 2450 MHz while measuring with box-horn designed at 2450 MHz. The spatial distribution of S_{21} parameter (transmission coefficient) and hence relative magnitude of electric-field in dB was registered by placing the co-axial monopole probe at different positions in synthetic muscle. Here, a coordinate system with the z-axis along the axis of the box-horn and perpendicular to the cross-section of the tissue model, and the x-y plane in the plane of the box-horn aperture has been considered with x-axis oriented in the direction of the electric field vector along the narrow dimension of the box-horn (Fig. 1). The measurement of the field components in synthetic muscle was carried out as given below. $E_x\,(x/y/z)$, i.e., spatial distribution of electric field in x-direction was measured by keeping monopole probe axis along x-direction and moving it in a desired direction (x- or y- or z-direction) keeping other coordinates fixed. This way E_x distributions along x-, y-, and z-directions were measured. Similarly, spatial distributions of E_y and E_z were also measured. The magnitude of field components E_y and E_z sampled by the probe along each of the x-, y-, and z-directions was very small in comparison to the magnitude of E_x in respective directions. The field components were sampled at a number of positions from 0 to ± 6 cm along each of the x- and y-directions and from 0 to 6 cm along z-direction for both the water-loaded box-horns applicators operating at 915 and 2450 MHz. The measured field components were converted into total electric field and then to specific absorption rate (SAR) by taking into account the thermal properties of the synthetic muscle utilizing Eqns. (24)–(25). The density [15] of muscle was taken equal to 1050 Kg/m^3 in the computation. The accuracy in the measurement of distance along the x-/y-/z-direction was 0.1 cm. The source frequency and S_{21} measurement accuracies of the vector network analyzer were equal to 0.0005% and 1 dB respectively. Although the probe position could not be measured to the degree of accuracy required for precision measurements, it was sufficient to prove the feasibility of this technique.

5. RESULTS AND DISCUSSION

The spatial distributions of relative SAR in bio-medium for water-loaded box-horn applicator designed at 915 and 2450 MHz are numerically computed from theoretical analytical model using MATLAB® and were measured experimentally with the help of Agilent/HP vector network analyzer (8714ET). The theoretical and

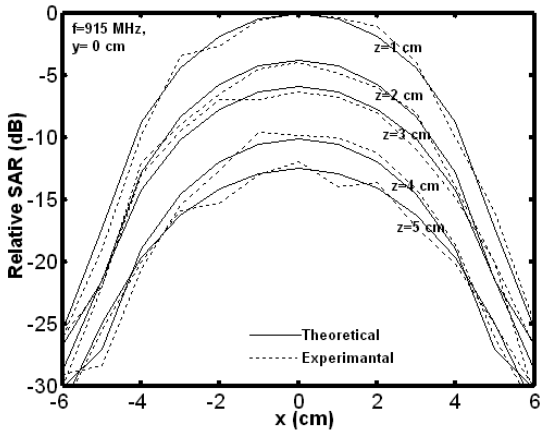

(a)

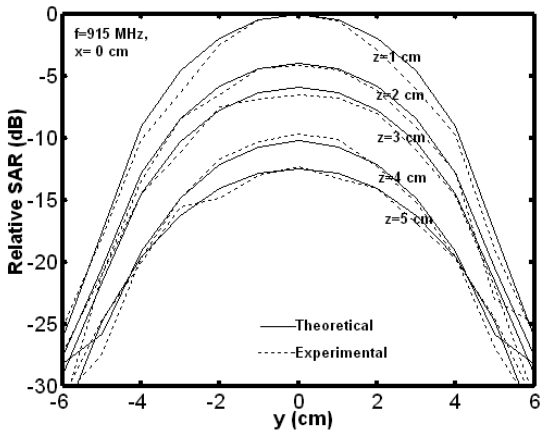

(b)

Figure 3. Comparison of theoretical and experimental relative SAR distribution in synthetic bio-medium heated by water-loaded box-horn at 915 MHz along (a) x-direction and (b) y-direction.

experimental heating patterns (SAR distributions) in the synthetic muscle model are compared for water-loaded box-horn applicator operating at 915 and 2450 MHz (Figs. 3–6). The theoretical and corresponding experimental results for SAR distributions are nearly in agreement with each other. Thus, the validity of the plane wave spectra technique is proved through measured SAR-distributions along the x-, y-, and z-directions for water-loaded box-horn applicators at 915 and

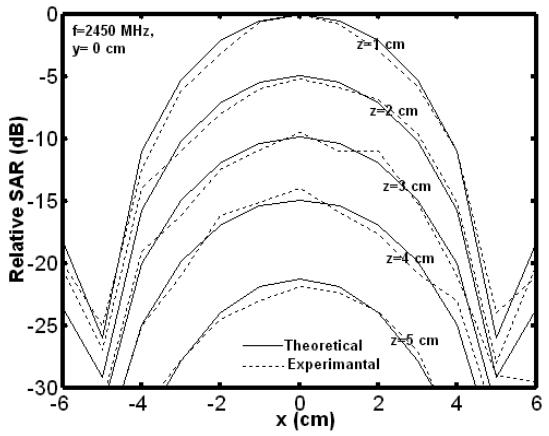

(a)

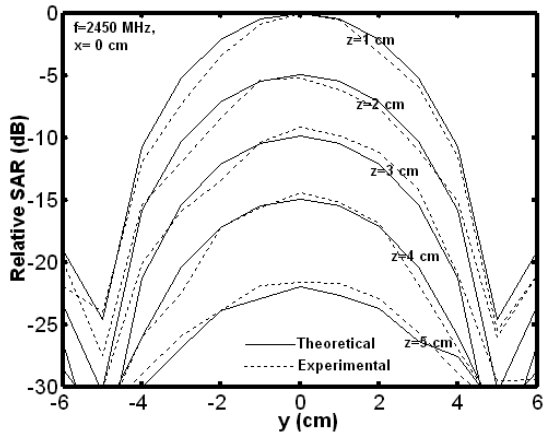

(b)

Figure 4. Comparison of theoretical and experimental relative SAR distribution in synthetic bio-medium heated by water-loaded box-horn at 2450 MHz along (a) x-direction and (b) y-direction.

2450 MHz. It is observed from Figs. 3–6 that experimental SAR values are deviating to a small degree from corresponding theoretical values. This mismatch may be due to the following factors. In theory, conducting ground plane surrounding the box-horn aperture extends upto infinity while in the developed box-horns finite size conducting ground plane has been taken. Therefore, small fringing field might have been present surrounding the box-horn apertures. There may

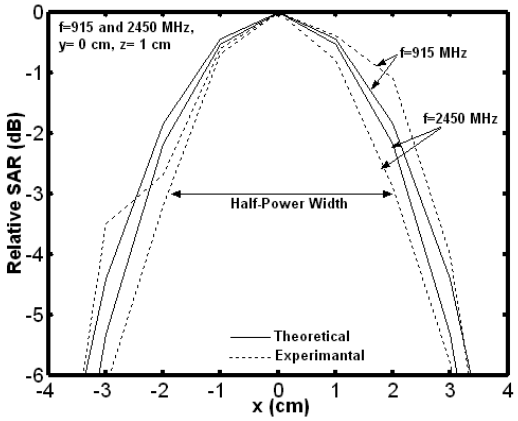

(a)

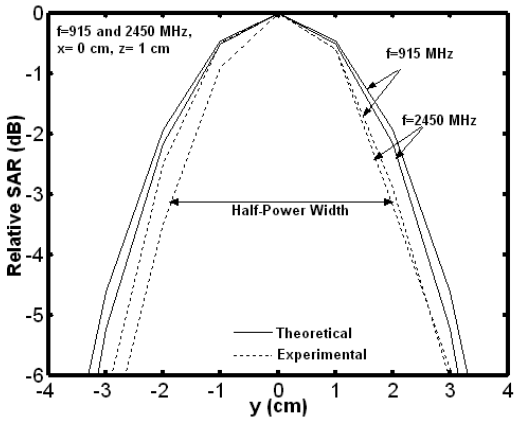

(b)

Figure 5. Relative SAR distribution in synthetic bio-medium heated by water-loaded box-horn at 915 and 2450 MHz along (a) x-direction and (b) y-direction, recasted and enlarged the portion of interest from Figures 3 and 4.

be evanescent modes excited near the discontinuity regions, such as the aperture of the box-horn which is neglected in the theoretical analysis. The accuracy of measuring the position of the monopole probe would also affect the accuracy of measured results. Interaction between the probe and the box-horn applicator may also occur. In actual practice some energy leakage from box-horn can also take place which is not considered in analysis. Although, these factors could cause

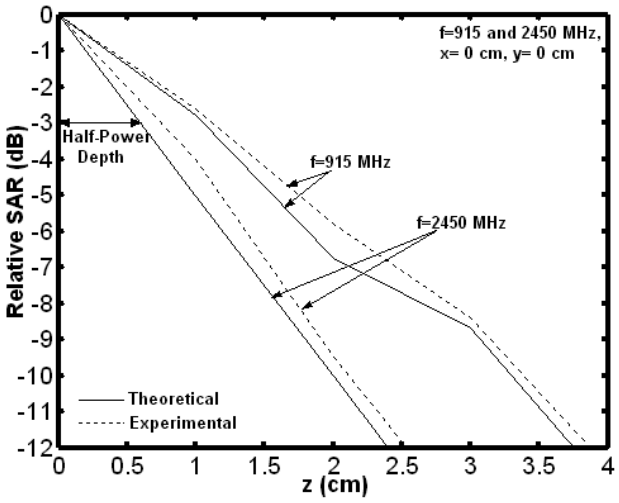

Figure 6. Comparison of theoretical and experimental relative SAR distribution in synthetic bio-medium heated by water-loaded box-horn at 915 and 2450 MHz along z-direction.

negligible effect on SAR-value independently but taken collectively may become significant and cause the mismatch between theoretical and experimental SAR values.

The normalized or relative SAR distributions (in dB) in synthetic-muscle layer produced by water-loaded box-horn operating at 915 MHz along x-/y-directions at different depths are presented in Fig. 3.

The spatial distributions of relative SAR in synthetic muscle medium in direct contact with water-loaded box-horn at 2450 MHz are depicted in Fig. 4. The SAR values in muscle layer are normalized to the maximum value of SAR that occurs in muscle.

The areas of interest from Figs. 3 and 4 are magnified and recasted in Fig. 5 for the sake of comparison between the half-power widths or resolutions of the applicators designed at 915 and 2450 MHz. The SAR distribution at 915 MHz is similar to that at 2450 MHz, but the distribution at 915 MHz is more spread spatially as compared to that at 2450 MHz. Therefore, the effective heating depends strongly on the frequency used and the field distribution across the aperture of the applicator.

Fig. 6 illustrates the results for a wave transmitted through planar stratified muscle medium in z-direction at 915 and 2450 MHz for water-loaded box-horn. The SAR value in muscle is normalized with respect

Table 1. Parameters of the box-horn applicators.

Parameters	Theoretical	Experimental	Theoretical	Experimental
Frequency (MHz)	915	915	2450	2450
Aperture size (cm^2)	1.26×5.94	1.26×5.94	0.43×2.23	0.43×2.23
Half-power width in x-direction(cm)	5.0	4.7	4.3	3.9
Half-power width in y-direction (cm)	5.0	4.2	4.3	3.8
Half-power depth in z-direction (cm)	1.1	1.2	0.6	0.7
Penetration depth in muscle (cm)	3.0	3.1	1.7	1.8
Power absorption coefficient (m^{-1})	33.32	32.26	58.82	55.56
Resolution (in x-/y-/z-direction) (relative)	low	low	high	high

to value at the box-horn-muscle interface. The penetration depth in muscle (depth where SAR value is down to 13.5 percent i.e., −8.7 dB of the maximum in the muscle) is given in Table 1 for box-horn applicators designed at 915 and 2450 MHz. The power absorption coefficient of muscle defined as inverse of penetration depth in muscle is also listed in Table 1 for 915 and 2450 MHz. Thus, at higher frequency, the dimensions of box-horn are compatible with localized treatment of tumor but penetration depth is less, whereas penetration depth is higher for applicator designed at lower frequency. The disadvantage of using lower frequency is the poor localization of heating because of increased dimension of the applicator. Thus, there is a trade off between penetration depth and localization. Also, the profile of wave penetration into the body is strongly dependent on frequency. To increase penetration depth further, box-horn can be arranged in phased array configuration. By dielectric-slab-loading in the centre of box-horn also, penetration depth can be improved. Integration of box-horn with metal-plate converging lens is another alternative to increase penetration depth. The applicators providing greater penetration depth can be used for deep-seated tumors.

The resolution of an applicator refers to its ability to resolve/distinguish two adjacent objects. Since two objects could be resolved if separated by a distance greater than the half-power

width/depth (shown in one of the curves each of Figures 5 and 6) of the SAR pattern, the half-power width/depth [16, 17] is conveniently referred to as the resolution of an applicator. Resolution in x- or y-direction can be expressed in terms of half-power width of the SAR distribution in muscle and resolution in z-direction can be expressed in terms of half-power depth of the SAR distribution in muscle. Higher resolution can be obtained by lower half-power width/depth (-3 dB width/depth) and vice-versa. The half-power widths in x- or y-direction and half-power depth in muscle extracted from Figures 5 and 6 at 915 and 2450 MHz are listed in Table 1. It can be concluded that the box-horn has lower resolutions in x-, y- and z-directions at 915 MHz as compared with corresponding resolutions at 2450 MHz. The resolution of box-horn depends on operating frequency. For hyperthermia application, the high SAR region should be limited to a smaller area (higher resolution) to avoid unnecessary damage to normal tissue. These requirements of the applicator can be achieved by employing box-horn in phased-array configuration.

6. CONCLUSION

A novel and efficient dual mode direct contact water-loaded box-horn applicator has been designed and developed and spatial patterns of SAR in muscle layer have been analyzed theoretically and measured at 915 and 2450 MHz. Hence, the technical feasibility of a safe and effective design of box-horn has been demonstrated. The water-loaded box-horn designed at 915 MHz gives higher penetration depth and lower resolution in muscle layer as compared with those for the horn designed at 2450 MHz. At higher frequencies where box-horn applicators of convenient size may be used to focus microwave energy within selected region of the body, the depth of penetration is so shallow that the energy cannot be directed efficiently into the deeper tissues. On the other hand, at lower frequencies where greater depth of penetration is obtained, the size of an applicator that is required to provide a focused beam becomes too large for practical clinical use. Therefore, a compromise must be made in the choice of frequency and the size of applicator so that a reasonable depth of penetration of energy can be achieved while, at the same time, the applicator should be restricted to a convenient size and weight for clinical use. The analysis and results presented here may be useful in designing and developing a novel, potential and highly efficient, dual-mode water-loaded box-horn applicator for uniform heating to prevent steep temperature gradient in bio-medium, and in analyzing the performance of the applicator for hyperthermia treatment of cancer.

ACKNOWLEDGMENT

The authors appreciate Mr. M. M. Sinha, Senior Technical Assistant, Center for Research in Microwave Tube (CRMT) workshop, IT-BHU, Varanasi, India for assisting in fabrication of the box-horn antennas and Dr. A. R. Harish, Assistant Professor, Indian Institute of Technology Kanpur (IIT Kanpur), India for his suggestions and providing facilities for experimental work. First author, R. C. Gupta wishes to acknowledge to the Department of Electronics Engineering, IT-BHU, Varanasi and UGC, New Delhi for awarding Senior Research Fellowship. Authors wish to thank the editorial board and reviewers for their invaluable suggestions to improve the quality of the paper.

REFERENCES

1. Guy, A. W., J. F. Lehmann, J. B. Stonebridge, and C. C. Sorenson, "Development of a 915-MHz direct-contact applicator for therapeutic heating of tissues," *IEEE Trans. Microwave Theory Tech.*, Vol. MTT-26, No. 8, 550–556, Aug. 1978.
2. Uzunoglu, N. K., E. A. Angelikas, and P. A. Cosmidis, "A 432 MHz local hyperthermia system using an indirectly cooled, water-loaded waveguide applicator," *IEEE Trans. Microwave Theory Tech.*, Vol. MTT-35, 106–111, 1987.
3. Verba, Jr., J., C. Franconi, F. Montecchia, and I. Vannucci, "Evanescent-mode applicators (EMA) for superficial and subcutaneous hyperthermia," *IEEE Trans. Microwave Theory Tech.*, Vol. MTT-40, 397–407, 1993.
4. Stuchly, M. A., S. S. Stuchly, and G. Kantor, "Diathermy applicators with circular aperture and corrugated flange," *IEEE Trans. Microwave Theory Tech.*, Vol. MTT-28, No. 3, 267–271, March 1980.
5. Lin, J. C., G. Kantor, and A. Ghods, "A class of new microwave therapeutic applicators," *Radio Sci.*, Vol. 17, 119s–124s, Sept.–Oct. 1982.
6. Samaras, T., P. J. M. Rietveld, and G. C. V. Rhoon, "Effectiveness of FDTD in predicting SAR distributions from the Lucite cone applicator," *IEEE Trans. Microwave Theory Tech.*, Vol. MTT-48, 2059–2063, Jan. 2000.
7. Nikawa, Y., H. Wantanabe, M. Kikuchi, and S. Mori, "A direct-contact microwave lens applicator with a microcomputer-controlled heating system for local hyperthermia," *IEEE Trans. Microwave Theory Tech.*, Vol. MTT-34, 626–630, May 1986.

8. Sherar, M. D., F. F. Liu, D. J. Newcombe, B. Cooper, W. Levin, W. B. Taylor, and J. W. Hunt, "Beam shaping for microwave waveguide hyperthermia applicators," *Int. J. Radiat. Oncol. Biol. Phys. (UK)*, Vol. 25, 849–857, 1993.
9. Alexander, P. H. and J. Liu, "Field analysis of dielectric-loaded lens applicator for microwave hyperthermia," *IEEE Trans. Microwave Theory Tech.*, Vol. MTT-41, 792–796, May 1993.
10. Compton, Jr., R. T., "The admittance of aperture antenna radiating into lossy media," Rep. 1691-5, Antenna Laboratory, Ohio State University, Research Foundation, Columbus, Ohio, 1964.
11. Harrington, R. F., *Time-harmonic Electromagnetic Field*, 123–135, McGraw-Hill Book Company, New York, 1961.
12. Silver, S. (ed.), *Microwave Antenna Theory and Design*, MIT Radiation laboratory series, Vol. 12, 123–135, McGraw-Hill Book Company, New York, 1949.
13. International Telephone and Telegraph Company, Reference data for radio engineers, 5/e, H. W. Sams & Company, Indianpolis, IN, 1968.
14. Stuchly, M. A. and S. S. Stuchly, "Dielectric properties of biological substances-tabulated," *J. Microwave Power*, Vol. 15, No. 1, 19–26, Jan. 1980.
15. Manson, P. A., W. D. Hurt, T. J. D'Andra, P. Gajšek, K. L. Ryan, D. A. Nelson, K. I. Smith, and J. M. Ziriax, "Effect of frequency, permittivity, and voxel size on predicted specific absorption rate values in biological tissue during electromagnetic field exposure," *IEEE Trans. Microwave Theory Tech.*, Vol. MTT-48, 2050–2058, Jan. 2000.
16. Loane, J., H. Ling, B. F. Wang, and S. W. Lee, "Experimental investigation of a retro-focused microwave hyperthermia applicator: Conjugate-field matching scheme," *IEEE Trans. Microwave Theory Tech.*, Vol. MTT-34, 490–494, May 1986.
17. Gee, W., S.-W. Lee, N. K. Bong, C. A. Cain, R. Mittra, and R. L. Magin, "Focused array hyperthermia applicator: Theory and experiment," *IEEE Trans. Biomed. Eng.*, Vol. BME-31, 38–46, Jan. 1984.